FORM and FORCE

Proceedings of the IASS Annual Symposium 2019 – Structural Membranes 2019
Form and Force
7–10 October 2019, Barcelona, Spain
C. Lázaro, K.-U. Bletzinger, E. Oñate (eds.)

Design of Novel Origami Shell Structures

Zeyuan He*, Simon D. Guest

* Department of Engineering, University of Cambridge
Trumpington Street, Cambridge CB2 1PZ, UK
zh299@cam.ac.uk

Abstract

A developable quadrilateral creased paper is the union of a planar region (the paper) and a quadrilateral mesh embedded on this paper. In this article we will present some design methods for constructing a shell structure based on three different types of rigid-foldable and developable quadrilateral creased papers. Each type mentioned in this article can approximate different types of surfaces. The first two types of quadrilateral creased papers also have the "self-locking" property – the rigid folding motion halts at the final rigidly folded states due to clashing of panels, and the final rigidly folded state forms the approximation. Each of the examples has a one degree of freedom unique rigid folding motion.

Keywords: rigid origami, rigid-foldability, approximation

1 Introduction

This paper will present some design methods for constructing a shell structure, which are based on different types of rigid-foldable and developable quadrilateral creased papers. A developable quadrilateral creased paper is the union of a planar region (the paper) and a quadrilateral mesh embedded on this paper.

Deployable shell structures are often considered for temporary shelters [1]. For such applications the shell structure needs to have the following properties: (1) enough structural strength and low self-weight (preferably portable by one person); (2) small packaged volume; (3) easily deployable (without the use of heavy lifting devices). It has been shown that origami has great potential for designing structures with those properties [1, 2], since (1) the rigid folded plates of these structures provide enhanced structural performance in the deployed form; (2) origami folds permit easy packaging in a small volume. Considering the design of an origami-inspired shelter, [3, 4] provide multi-objective shape optimization methodologies which balance the priorities of structural performance and energy efficiency, including dimension control and material selection. Some other shape design methods and shelter examples can be seen in [5, 6]. Based on the shape provided by origami design, it will then be possible for soft wall (canvas) and rigid wall solutions to be packaged, assembled, deployed and fixed to become a practical shelter.

In this paper we will enlarge the range of possible design of such shell structures by applying the techniques developed in [7] and considering new types of rigid-foldable quadrilateral creased paper. Here three design examples for a shell structure, each based on one of these types, will

be discussed in detail. The first example is the developable case of the "parallel repeating" type, which is generated with rows of parallel inner creases; the second one is the developable case of the "orthodiagonal" type, which is generated with several parallel straight line segments; and the third one is the developable case of the "longitudinal linear repeating" type, which is newly discovered [8] and has less regular rigid folding motion than the other two types.

2 Design Method with the Parallel Repeating Type

In this section we will present the design method for the parallel repeating type of rigid-foldable quadrilateral creased paper. This method can generate an approximation to a surface where a planar target curve f is scanned along a planar datum curve g. The angle between the plane containing f and the tangent vector of g, can be adjusted. With given f and g, an example of the parallel repeating type is shown in Figure 1(a). Here all the rows of inner creases are parallel, and all the columns are straight lines. If the number of inner vertices in the longitudinal and transverse directions are m (m is odd) and n, there are $m+2$ parallel rows and $n+2$ straight line columns in the crease pattern. In Figure 1(b), the second left column (colored green) approximates f at the final rigidly folded state, and the middle row (colored red) approximates g at the final rigidly folded state. Note that the first and last column of panels are designed to halt the rigid folding motion by clashing of panels. Then the geometric parameters of the crease pattern are the sector angles on the middle row, and the length of all the inner creases colored red and green.

The algorithm to determine the above geometric parameters are listed below.

(1) From the creased paper we choose, the target curve $f : I \ni t \to (x(t), y(t)) \in \mathbb{R}^2$ is approximated by a polyline, and the angle ξ between adjacent line segments is constant (Figure 1(c)). In order to be approximated, f should satisfy the following condition: there exists a rotation $\theta \in [0, 2\pi)$ and a shear transformation of magnitude $\pi/2 - \xi$, $\xi \in [0, \pi]$, s.t. after the affine transformation $f \to \overline{f}$ described below, $\overline{f}$ is monotone decreasing.

$$\begin{bmatrix} \overline{x}(t) \\ \overline{y}(t) \end{bmatrix} = \begin{bmatrix} 1 & -1/\tan\xi \\ 0 & 1/\sin\xi \end{bmatrix} \begin{bmatrix} \cos\theta & \sin\theta \\ -\sin\theta & \cos\theta \end{bmatrix} \begin{bmatrix} x(t) \\ y(t) \end{bmatrix} \tag{1}$$

The proof of this condition and the approximation of f based on the above shear transformation are provided in Proposition 2 of [7]. With ξ chosen, the length of inner creases colored green d_i ($1 \le i \le m+1$) can be obtained.

(2) Approximate g by a polyline (Figure 1(d)), then the lengths of inner creases colored red l_i ($1 \le i \le n-1$) can be obtained. Consider the projection of the plane containing each column of inner creases, the angles between these projections and each line segment of the polyline (measured from the same side) are named δ_i ($1 \le i \le 2n-2$), which can be calculated directly. In Figure 1(d) all the projections are perpendicular to the tangent vector of g, but other choices are also possible.

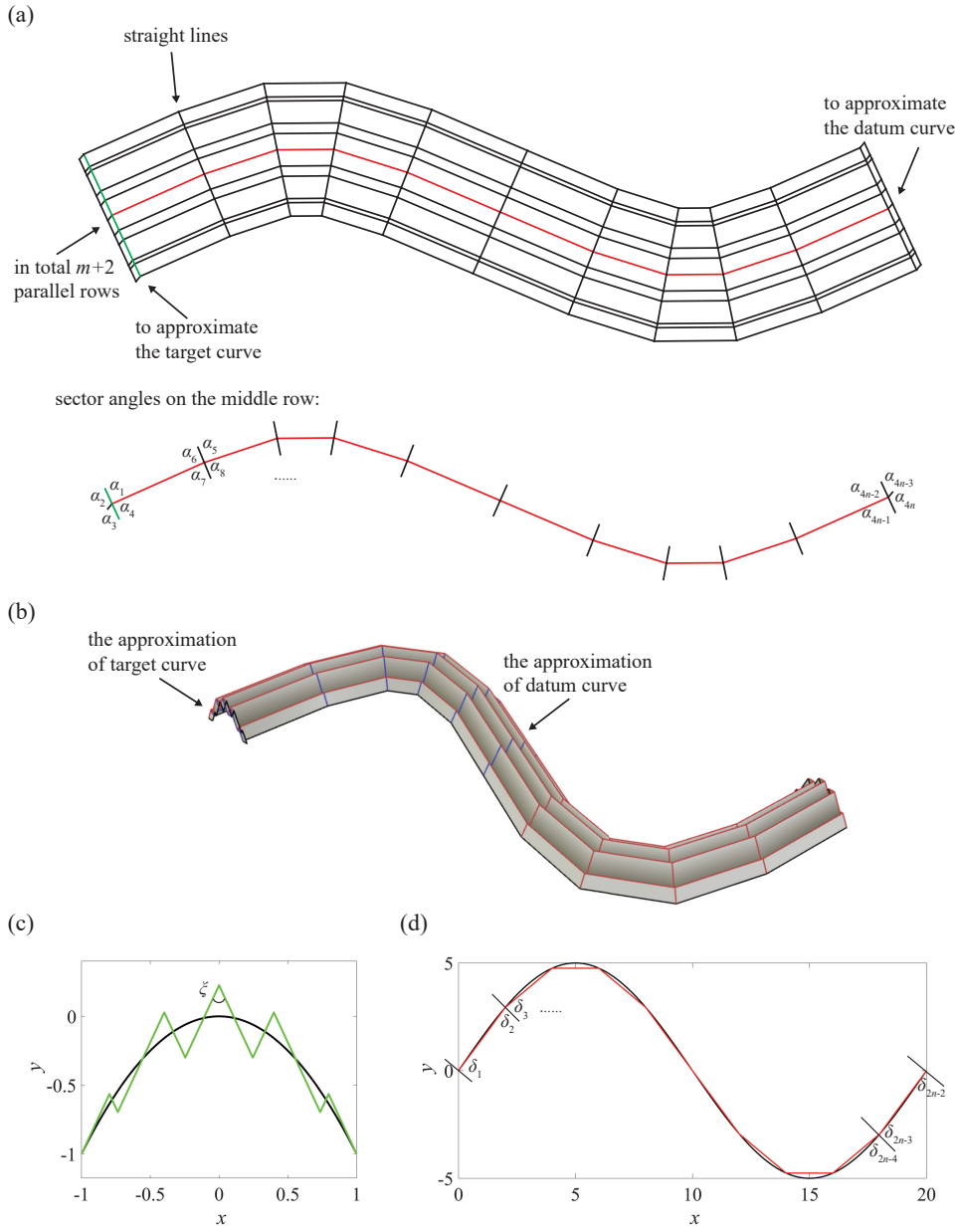

Figure 1: The approximation of the parallel repeating type. (a) shows the crease pattern. Here all the rows of inner creases are parallel, and all the columns are straight lines. There are $m = 9$ rows and $n = 11$ columns of inner vertices. The second left column (colored green) approximates the target curve $f = -x^2$ $(-1 \le x \le 1)$ at the final rigidly folded state, and the middle row (colored red) approximates the datum curve $g = 5\sin(\pi x/10)$ $(0 \le x \le 20)$ at the final rigidly folded state. (b) shows the approximation, where the first and last column of panels are designed to halt the rigid folding motion by clashing of panels. This figure is plotted by Freeform Origami [2], where the mountain and valley creases are colored red and blue. (c) is the approximation of the target curve (colored green). Here the angle ξ between adjacent line segments is constant. (d) is the approximation of the datum curve (colored red). Consider the projection of the plane containing each column of inner creases, the angles between these projections and each line segment of the polyline (measured from the same side) are named δ_i $(1 \le i \le 2n-2)$.

(3) Calculate all the sector angles on the middle row α_i $(1 \leq i \leq 4n)$:

$$\begin{aligned}
\alpha_3 &= \frac{\pi - \xi}{2} \\
|\cos\alpha_4| &= \cos\delta_1 \cos\alpha_3 \\
\frac{\tan\alpha_{4i+3}}{\tan\delta_{2i}} &= \frac{\tan\alpha_{4i}}{\tan\delta_{2i-1}} \ (1 \leq i \leq n-1) \\
\frac{\cos\alpha_{4i+4}}{\cos\delta_{2i+1}} &= \frac{\cos\alpha_{4i+3}}{\cos\delta_{2i}} \ (1 \leq i \leq n-2) \\
|\cos\alpha_{4n}| &= \frac{\cos\alpha_{4n-1}}{\cos\delta_{2n-2}} \\
\alpha_{4i-3} &= \pi - \alpha_{4i} \ (1 \leq i \leq n) \\
\alpha_{4i-2} &= \pi - \alpha_{4i-1} \ (1 \leq i \leq n)
\end{aligned} \tag{2}$$

(4) With α_i $(1 \leq i \leq 4n)$, d_i $(1 \leq i \leq m+1)$ and l_i $(1 \leq i \leq n-1)$, draw the creased paper.

From direct geometric analysis, at the jth $(2 \leq j \leq n)$ column of inner creases, the angle between adjacent inner creases is not ξ. However, we can still write the curve approximated by the nth column as an affine transformation of f, which is given in [7]. If $m, n \to \infty$, the approximation from each column will become f, hence this type can approximate a surface where a planar target curve f is scanned along a planar datum curve g.

3 Design Method with the Orthodiagonal Type

In this section we will present the design method for the orthodiagonal type. This method can approximate a cylindrical developable surface where a planar target curve f is scanned along a planar datum curve g. Here each column or row of inner creases are co-planar, and each plane containing a column of inner creases is orthogonal to each plane containing a row of inner creases. With given f and g, an example of the orthodiagonal type is shown in Figure 2(a). All the columns are straight lines and parallel to each other, and the sector angles in different rows satisfy certain equations. If the number of inner vertices in the longitudinal and transverse directions are m (m is odd) and n, there are $m+2$ rows and $n+2$ straight line columns in the crease pattern. In Figure 2(b), the second left column (colored green) approximates f at the final rigidly folded state, and the middle row (colored red) approximates g at the final rigidly folded state. Note that the first and last column of panels are designed to halt the rigid folding motion by clashing of panels. Then the geometric parameters of the crease pattern are all of the sector angles, and the length of all the inner creases colored red and green.

The algorithm to determine the above geometric parameters is listed below.

(1) Approximate f by a polyline (Figure 1(c)) which turns left and right alternately. Thus the lengths of inner creases colored green d_i $(1 \leq i \leq m+1)$ can be obtained. Then calculate the angle between adjacent line segments β_i (measured from the alternating sides, $1 \leq i \leq m$).

(2) Approximate g by a polyline, and find the lengths of inner creases colored red l_i $(1 \leq i \leq n-1)$. Calculate the angle between adjacent line segments γ_i (measured from the same side, $1 \leq i \leq n-2$).

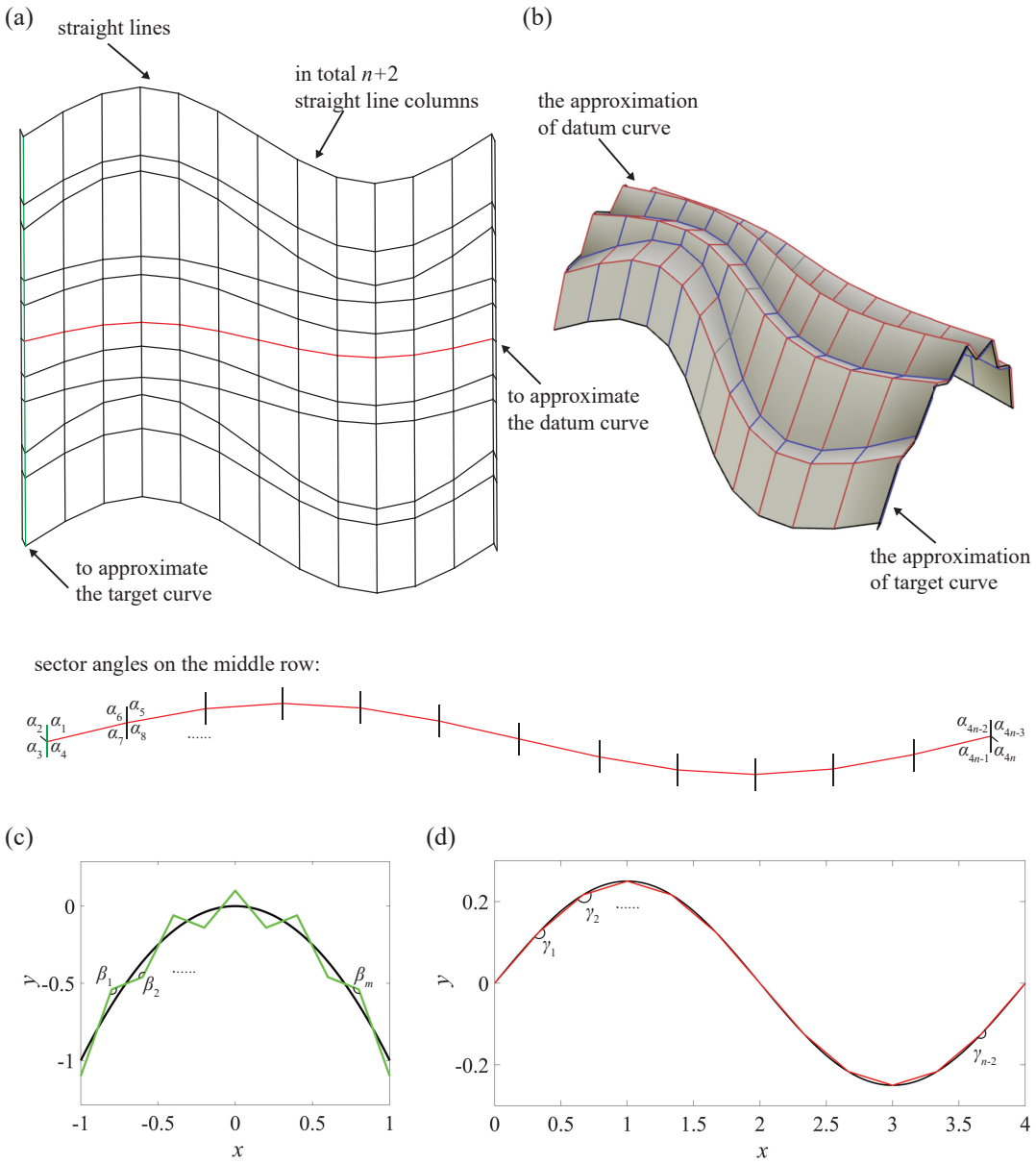

Figure 2: The approximation of the orthodiagonal type. (a) shows the crease pattern. Here each column or row of inner creases are co-planar, and each plane containing a column of inner creases is orthogonal to each plane containing a row of inner creases. There are $m = 9$ rows and $n = 13$ columns of inner vertices. The second left column (colored green) approximates the target curve $f = -x^2$ $(-1 \leq x \leq 1)$ at the final rigidly folded state, and the middle row (colored red) approximates the datum curve $g = 0.25\sin(\pi x/2)$ $(0 \leq x \leq 4)$ at the final rigidly folded state. (b) shows the approximation, where the first and last column of panels are designed to halt the rigid folding motion by clashing of panels. This figure is plotted by Freeform Origami [2], where the mountain and valley creases are colored red and blue. (c) is the approximation of the target curve (colored green). The angles between adjacent line segments are β_i $(1 \leq i \leq m)$, which are measured from the alternating sides. (d) is the approximation of the datum curve (colored red). The angles between adjacent line segments are γ_i $(1 \leq i \leq n-2)$, which are measured from the same side.

(3) Choose α_0 s.t. $\pi/2 < \alpha_0 < (\pi + \beta_{(m+1)/2})/2$, then calculate all the sector angles α_{ij} $(1 \le i \le m, 1 \le j \le 4n)$, α_0 controls the angle between the tangent vector of g and the plane containing f:

$$\begin{gathered}
\alpha_{i,3} = \alpha_{i,4n} = \frac{\pi + \beta_i}{2} \ (1 \le i \le m) \\
\alpha_{(m+1)/2,4} = \alpha_0 \\
\alpha_{(m+1)/2,4j-1} = \pi - \alpha_{(m+1)/2,4j-4} \ (2 \le j \le n) \\
\frac{\cos\alpha_{(m+1)/2,4j}}{|\cos\alpha_{(m+1)/2,3}|} = \cos(\gamma_{j-1} - \arccos\frac{\cos\alpha_{(m+1)/2,4j-1}}{|\cos\alpha_{(m+1)/2,3}|}) \ (2 \le j \le n-1) \\
\frac{\tan\alpha_{i,4j}}{\tan\alpha_{i+1,4j}} = \frac{\tan\alpha_{i,4j-1}}{\tan\alpha_{i+1,4j-1}} \ (\frac{m-1}{2} \ge i \ge 1, 1 \le j \le n-1) \\
\alpha_{i,4j+3} = \pi - \alpha_{i,4j} \ (\frac{m-1}{2} \ge i \ge 1, 1 \le j \le n-1) \\
\frac{\tan\alpha_{i,4j}}{\tan\alpha_{i-1,4j}} = \frac{\tan\alpha_{i,4j-1}}{\tan\alpha_{i-1,4j-1}} \ (\frac{m+3}{2} \le i \le m, 1 \le j \le n-1) \\
\alpha_{i,4j+3} = \pi - \alpha_{i,4j} \ (\frac{m+3}{2} \le i \le m, 1 \le j \le n-1) \\
\alpha_{i,4j-3} = \pi - \alpha_{i,4j} \ (1 \le i \le m, 1 \le j \le n) \\
\alpha_{i,4j-2} = \pi - \alpha_{i,4j-1} \ (1 \le i \le m, 1 \le j \le n)
\end{gathered} \tag{3}$$

(4) With α_i $(1 \le i \le 4n)$, d_i $(1 \le i \le m+1)$ and l_i $(1 \le i \le n-1)$, draw the creased paper.

From direct geometric analysis, at the jth $(2 \le j \le n)$ column of inner creases, the angle between adjacent inner creases is still β. We can also write the curve approximated by the nth column as an affine transformation of f, which is given in [7]. If $m, n \to \infty$, the approximation from each column will become f, and since the planes containing each column are parallel, this type can approximate a cylindrical developable surface that a planar target curve f is scanned along a planar datum curve g.

4 Design Method with the Longitudinal Linear Repeating Type

In this section we will introduce the design example for the new type of rigid-foldable quadrilateral creased paper, as shown in Figure 3(a). Here the input sector angles are $\alpha_1, \beta_1, \gamma_1, \delta_1 \in (0, \pi)$ (colored red). We can solve $\alpha_2, \beta_2, \gamma_2, \delta_2$ numerically from the four equations in (4), and hence all the sector angles in Figure 3(a) are known. These equations are derived in [9].

The next step is to tessellate the sector angles in Figure 3(a) to generate a infinitely extendable rigid-foldable quadrilateral creased paper. It is possible to adjust the length of a row (colored red) and a column (colored green) of inner creases. These lengths are required to fully determine the creased paper once the input sector angles are given. In each row, the sector angles repeat every four columns of inner vertices; in each column, the sector angles repeat every two rows of inner vertices. Note that each row of inner creases are co-planar thoughout the folding, while each column of inner creases are not co-planar. For this new type of crease pattern, it is unclear how we can describe the surface that can be approximated. One possibility is to approximate a target curve f scanning along a line g, where the curvature of f will increase or decrease monotonously. We provide an example in Figure 3(b), where f is approximately an arc.

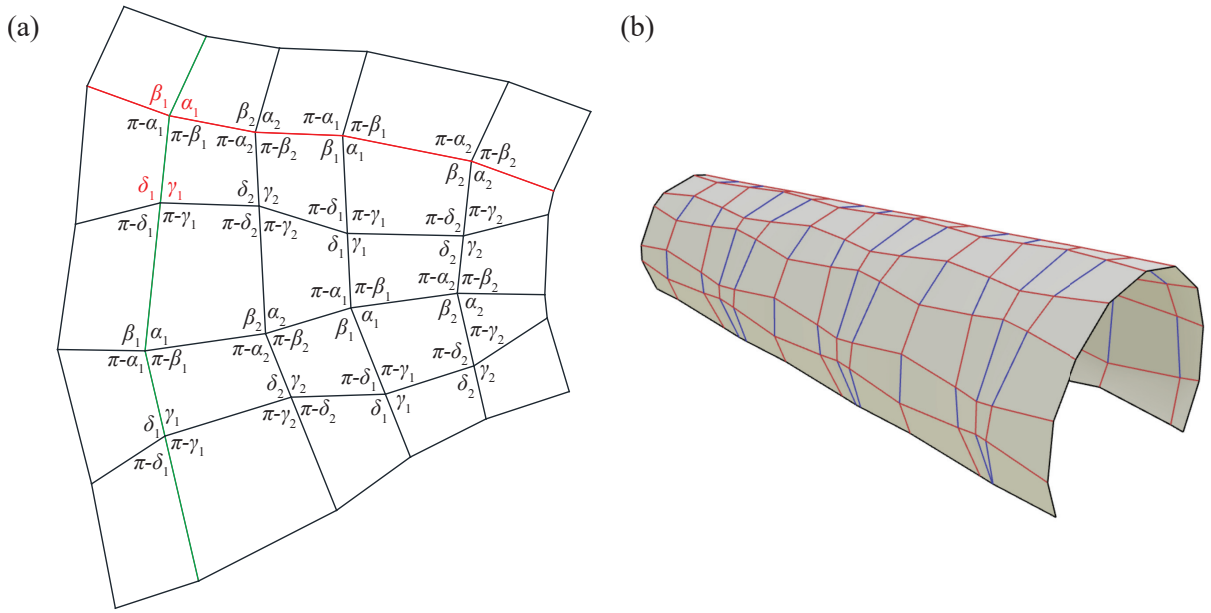

Figure 3: The longitudinal linear repeating type. (a) illustrates the relation among the sector angles, where the input sector angles $\alpha_1, \beta_1, \gamma_1, \delta_1$ are colored red, and $\alpha_2, \beta_2, \gamma_2, \delta_2$ are solved numerically. All the sector angles and the length of a row (colored red) and a column (colored green) of inner creases determine the entire creased paper. In each row, the sector angles repeat every four columns of inner vertices; in each column, the sector angles repeat every two rows of inner vertices. (b) is an approximation of a circular shell, where the radius of the cross section r mototonously increases to $1.67r$. Here the sector angles are $\alpha_1 = 85°, \beta_1 = 80°, \gamma_1 = 95°, \delta_1 = 100°$; $\alpha_2 = 91.23°, \beta_2 = 86.23°, \gamma_2 = 106.23°, \delta_2 = 76.23°$. The length of inner creases on the second left column are set to be equal. The length of inner creases on the middle row is randomly chosen. (b) is plotted by Freeform Origami [2], where the mountain and valley creases are colored red and blue.

$$\begin{aligned}
\beta_1 + \alpha_2 - \gamma_1 - \delta_2 &= 0 \\
\alpha_1 + \beta_2 - \gamma_1 - \delta_2 &= 0 \\
\sin\gamma_1 \sin\gamma_2 - \sin\delta_1 \sin\delta_2 &= 0
\end{aligned}$$

The last equation can be chosen from

$$c = \frac{\sin\dfrac{\alpha_1 - \beta_1}{2} \sin\dfrac{\beta_2 + \alpha_2}{2}}{\sin\dfrac{\alpha_1 + \beta_1}{2} \sin\dfrac{\beta_2 - \alpha_2}{2}} = k\sqrt{\frac{\sin(\delta_2 + \gamma_2)\sin(\gamma_1 - \delta_1)}{\sin(\delta_2 - \gamma_2)\sin(\gamma_1 + \delta_1)}}$$

or

$$\begin{aligned}
c = \frac{\cos\dfrac{\alpha_1 - \beta_1}{2} \cos\dfrac{\beta_2 + \alpha_2}{2}}{\cos\dfrac{\alpha_1 + \beta_1}{2} \cos\dfrac{\beta_2 - \alpha_2}{2}} &= k\sqrt{\frac{\sin(\delta_2 + \gamma_2)\sin(\gamma_1 - \delta_1)}{\sin(\delta_2 - \gamma_2)\sin(\gamma_1 + \delta_1)}} \\
k = 1 \quad \text{if} \quad (\gamma_1 + \delta_1 - \pi)(\gamma_2 + \delta_2 - \pi) &> 0 \\
k = -1 \quad \text{if} \quad (\gamma_1 + \delta_1 - \pi)(\gamma_2 + \delta_2 - \pi) &< 0
\end{aligned} \tag{4}$$

Remark 1. The design example shown in Figure 3(a) is a periodical solution of the longitudinal linear repeating type in [8], but is not the only case. It is possible to get some non-perodical solutions numerically, and the rigidly folded states can reach some other shapes. Since equation (4) is highly non-linear, there might be no solution or only degenerated solutions for a given set of input sector angles.

5 Conclusion

This paper demonstrates three methods to approximate different types of surfaces based on the developable case of three types of rigid-foldable quadrilateral creased papers. For the first two types, the first and last column of panels are designed to halt the rigid folding motion by clashing of panels. All the quadrilateral creased papers used in this paper have a unique one degree of freedom rigid folding motion.

References

[1] A. P. Thrall and C. P. Quaglia, "Accordion shelters: A historical review of origami-like deployable shelters developed by the US military," *Engineering structures*, 59:686–692, 2014.

[2] Tomohiro Tachi, "Freeform rigid-foldable structure using bidirectionally flat-foldable planar quadrilateral mesh," *Advances in architectural geometry*, pages 87–102, 2010.

[3] F. J. Martínez-Martín and A. P. Thrall, "Honeycomb core sandwich panels for origami-inspired deployable shelters: Multi-objective optimization for minimum weight and maximum energy efficiency," *Engineering Structures*, 69:158–167, 2014.

[4] C. P. Quaglia, N. Yu, A. P. Thrall, and S. Paolucci, "Balancing energy efficiency and structural performance through multi-objective shape optimization: Case study of a rapidly deployable origami-inspired shelter," *Energy and Buildings*, 82:733–745, October 2014.

[5] Ting-Uei Lee and Joseph M. Gattas, "Geometric design and construction of structurally stabilized accordion shelters," *Journal of Mechanisms and Robotics*, 8(3):031009, 2016.

[6] Niels De Temmerman, Marijke Mollaert, Tom Van Mele, and Lars De Laet, "Design and analysis of a foldable mobile shelter system," *International Journal of Space Structures*, 22(3):161–168, 2007.

[7] Zeyuan He and Simon D. Guest, "Approximating a Target Surface with 1-DOF Rigid Origami," *in Origami 7: The proceedings from the seventh meeting of Origami, Science, Mathematics and Education*, volume 2, pages 505–520. Tarquin, 2018.

[8] Zeyuan He and Simon D. Guest, "On Rigid Origami II: Quadrilateral Creased Papers," *arXiv preprint arXiv:1804.06483*, 2018.

[9] Ivan Izmestiev, "Classification of flexible Kokotsakis polyhedra with quadrangular base," *International Mathematics Research Notices*, 2017(3):715–808, 2017.